

# MEDIRAD

**Project title: Implications of Medical Low Dose Radiation Exposure**

Grant Agreement Number: 755523

Call identifier: NFRP-2016-2017

Topic: NFRP-9

## **Deliverable D3.9**

### **Report on the use of the DNA damage assay to determine radiosensitivity in patients**

**Lead partner:** UKW

**Author(s):** S. Schumann, U. Eberlein, P. Hartrampf, N. Hasenauer, A.K. Buck, M. Lassmann – University Hospital Würzburg, Würzburg Germany (UKW)  
K. Pfestroff, A. Pfestroff, M. Luster – University Hospital Marburg, Marburg Germany (UMR)  
M. Port, H. Scherthan – Bundeswehr Institute of Radiobiology, Munich, Germany

**Work Package:** WP3

**Estimated delivery:** 28-Sep-2021

**Actual delivery:** 28-Sep-2021

**Type:** Report

**Dissemination level:** Public

*This project has received funding from the Euratom research and training programme 2014-2018 under grant agreement No 755523.*



## Table of contents

List of figures .....	2
List of tables .....	2
Abbreviations .....	2
1. Introduction.....	3
2. Material and Methods.....	4
2.1 Patients .....	4
2.2 Blood sampling and activity determination of blood samples in patients .....	5
2.3 Blood sample preparation for the DNA damage focus assay .....	5
2.4 Measurement of the whole-body retention.....	5
2.5 Calculation of the time-integrated activity coefficients and the absorbed doses for blood-based dosimetry.....	5
2.6 Statistical analysis .....	6
3. Results .....	6
3.1 Patients .....	6
3.2 Ex-vivo data on DNA damage induction and repair.....	7
3.3 In-vivo data on DNA damage induction and repair in patients .....	9
3.3.1 Blood-based dosimetry .....	9
3.3.2 DNA damage induction and repair.....	10
3.3.3 Comparison of in-vivo and ex vivo-repair .....	12
4. Conclusion .....	14
5. References.....	15

## List of figures

Figure 1: Box plot of the average number of RIF per cell immediately after, 4 h and 24 h after ex-vivo irradiation with 50 mGy. The boxes comprise the 2<sup>nd</sup> and 3<sup>rd</sup> quartile of the data, the horizontal line defines the median and the circle the mean. Outliers ( $> 1.5 \times \text{IQR}$  (interquartile range)) are marked by filled diamonds.

Figure 2: Time course of the average number of RIF per cell after administration of <sup>131</sup>I in 18 patients IP1-IP18 shown as a box plot including the data points and the corresponding fit of a normal distribution as a black dotted line.

Figure 3: Average number of RIF/cell as a function of the absorbed dose to the blood. For the time points up to 5 h after administration a linear fit is denoted by a straight line (grey area: 95 % confidence band (CB)).

Figure 4: Average number of RIF/cell at time points  $> 24$  h as a function of the absorbed dose rate to the blood. A linear fit is denoted by a straight line (grey area: 95 % confidence band (CB)).

Figure 5: Comparison of the ex vivo (left panel A) and in vivo (right panel B) repair dynamics as a function of time after irradiation (ex vivo) or radioiodine administration (in vivo). In addition, panel B shows the mean absorbed doses to the blood at the nominal time points. The boxes comprise the 2<sup>nd</sup> and 3<sup>rd</sup> quartile of the data, the horizontal line defines the median and the circle the mean. Outliers ( $> 1.5 \times \text{IQR}$ ) are marked by filled diamonds.

## List of tables

Table 1: Patient coding and demographic data.

Table 2: Mean values of absorbed doses and dose rates to the blood at the nominal time points of blood sampling.

## Abbreviations

CB: Confidence band

[<sup>131</sup>I]NaI: Radioiodine

IQR: Interquartile range

RIF: Radiation-induced foci

UKW: University Hospital Würzburg

UMR: University Hospital Marburg

## 1. Introduction

The role of task 3.4 of WP3 was to determine quantitatively, ex vivo and in vivo, the DNA damage in peripheral blood mononuclear cells (PBMCs) induced by  $^{131}\text{I}$  as a measure of the absorbed dose and sensitivity. As biomarkers,  $\gamma\text{-H2AX}$  and 53BP1 were used to quantify the absorbed dose-dependent induction and repair of radiation damage to the DNA (“DNA damage assay”).

For the ex-vivo study of DNA damage induction and repair, 30 consenting patients were supposed to be included. Pre-administration blood samples should be obtained, irradiated internally ex vivo, by adding  $^{131}\text{I}$  solution to the blood. Afterwards the samples are processed according to a common protocol, anonymized and sent to the Bundeswehr Institute of Radiobiology in Munich for further processing and quantification of DNA damage. The measure for DNA damage is the number of colocalized ( $\gamma\text{-H2AX}$  and 53BP1) radiation-induced foci per cell (RIF).

For the in-vivo study, for 20 of these patients, treated at UKW, multiple blood samples should be acquired immediately in the first hours and up to 7 days after  $^{131}\text{I}$  administration and processed for analysis the same way as for the ex-vivo study.

The DNA damage assay will be used as a marker of the absorbed dose to the blood and it should be used as marker of inter-patient differences in radiosensitivity by assessing the persistence in time of the colocalizing  $\gamma\text{-H2AX}+53\text{BP1}$  foci over time as a measure of rate of DNA damage repair.

## 2. Material and Methods

### 2.1 Patients

The common study protocol was presented to the local ethics committees of the Medical Faculty of the University of Würzburg (UKW) and Marburg (UKM) and approved. All procedures performed in this study involving human participants were in accordance with the ethical standards of the respective ethics committees (UKW: Az. 246/18, UKM: Az. 83/19) and with the principles of the 1964 Declaration of Helsinki and its later amendments or comparable ethical standards. Informed consent was obtained from all individual participants included in the study.

**The inclusion criteria for participating in the study were as follows:**

- Able and willing to give signed informed consent
- Age  $\geq$  18 years
- Total thyroidectomy performed within a maximum of 6-8 weeks before radioiodine treatment
- Histological evidence for differentiated thyroid carcinoma (DTC) (papillary, follicular variants). Histological variants of aggressive disease such as tall cell, columnar, hobnail, diffuse sclerosing variants will be excluded.
- Tumor staging: pT1a(m) N0, T1aN1 or unfavorable histological characteristics (diffuse sclerosing, tall cell, hobnail variant), T1bN0-1, T2N0-1, T3aN0-1 (in accordance with the 8<sup>th</sup> ed. of the AJCC/UICC TNM staging, 2017, [1]).
- No distant metastases
- Clinical indication for [<sup>131</sup>I]NaI therapy as determined by the attending physician based on the available clinical information
- WHO score, ECOG score 0-2 (autonomous, self-caring)
- No history of prior therapeutic radiation / radionuclide exposure
- No history of chemotherapy
- No medication known to interfere with iodine kinetics within the last 12 months
- No amiodarone exposure in the last 24 months
- No exposure to iodinated contrast agent in the last six months
- No hemodialysis

**Patients were excluded if they did meet the following criteria:**

- Pregnancy (to be excluded by serum beta-HCG measurement in women of child-bearing age)
- Lactation within the last 6 months
- Participation in another clinical study within the last 6 months
- Current uncontrolled severe disease
- History of prior malignancy with the exception of low-grade skin cancer
- Inability to tolerate the necessary measurements for the study

**Additional exclusion criteria for the biodosimetry study were:**

- Diseases of the hematopoietic system
- Diagnostic exposure to ionizing radiation within one week of planned exposure to <sup>131</sup>I

Prior to the study, all patients gave their informed consent. For thyroid ablation treatment, the patients were hospitalized for at least 48 hours, normally up to 3-4 days.

## 2.2 Blood sampling and activity determination of blood samples in patients

Blood samples were taken from all patients using Li-Heparin blood collecting tubes (S-Monovette, Sarstedt, Germany). For the determination of the individual background focus rate and for the irradiation ex vivo samples were obtained prior to administration of radioiodine. For the patients treated at UKW, samples after administration were obtained at 1 h, 2 h, 3 h, 4 h, 24 h, 48 h, 96 h and up to 168 h. After the corresponding blood collection, PBMCs were isolated by density centrifugation in CPT tubes (BD) and directly fixed in 70% ethanol and stored at -20°C until DNA damage evaluation.

For determining the DNA damage induced by internal irradiation ex vivo, the blood samples taken before therapy were irradiated by addition of  $^{131}\text{I}$  solution, resulting in absorbed doses to the blood of nominal 50 mGy after 1 h incubation on a roller mixer at 37°C. One part of the sample taken before administration remained unirradiated for determination of background DNA damage foci. To investigate DNA damage repair ex vivo, the PBMCs isolated from the irradiated blood samples were split in three parts and either fixed directly (d) or after 4 h or 24 h culture in RPMI medium at 37°C.

For an exact quantification of the blood activity concentration, an aliquot of each heparinized blood sample was measured in a high-purity germanium detector (Canberra, Germany). The counting efficiencies of the detectors was determined by repeated measurements of a NIST-traceable standard. The measured values were decay-corrected to the time of blood drawing.

## 2.3 Blood sample preparation for the DNA damage focus assay

The separation and fixation of the PBMCs and the evaluation of colocalizing  $\gamma\text{-H2AX}+53\text{BP1}$  foci followed the protocol described in detail by Eberlein et al. [2]. Briefly, PBMCs were separated by density centrifugation in BD Vacutainer CPT tubes (BD, Heidelberg, Germany), washed in PBS, fixed in 70% ethanol and stored at -20°C. Immunofluorescence staining and foci analysis [3] was performed in the Bundeswehr Institute of Radiobiology in Munich, Germany. Generally, colocalizing  $\gamma\text{-H2AX}+53\text{BP1}$  foci were counted manually in 100 cells per sample. The individual background focus rate that was obtained by evaluating the non-irradiated samples before therapy start, was subtracted from the foci counts obtained after irradiation, which resulted in the average number of RIF per cell.

## 2.4 Measurement of the whole-body retention

Whole body activity retention was determined in all patients treated at UKW by external dose rate measurements and whole-body scans. Dose-rate measurements were performed by use of a ceiling-mounted shielded survey meter (automess GmbH, Germany) at a fixed distance of 2.5 m above the patients' beds. The first patient measurement was carried out immediately after administration (generally 5 to 30 minutes after  $^{131}\text{I}$ NaI application) and at least two times per day thereafter. Data were normalized to the first initial measurement.

The whole-body scans were performed at the nominal time points defined by the clinical protocol 4 h, 24 h, 48 h, 72 h, 96 h and 168 h post administration of  $^{131}\text{I}$ NaI.

## 2.5 Calculation of the time-integrated activity coefficients and the absorbed doses for blood-based dosimetry

The calculation of the time-dependent time-integrated activity coefficients for the total body ( $\tau_{\text{tb}}(t)$ ) and the blood ( $\tau_{\text{ml of bl}}(t)$ ) and the absorbed doses to the blood ( $\bar{D}_{\text{bl}}(t)$ ) after administration of  $^{131}\text{I}$  were performed according to the EANM SOP [4] and as described previously [5]. Since we took multiple

blood samples and measured the retention of the whole-body up to 168 h after therapy, the time-activity curves for  $^{131}\text{I}$  were fitted by bi-exponential functions.

As the activity was administered orally, the iodine washout from the stomach to the blood circulation needs to be taken into account. According to Leggett [6], the iodine uptake is 5% per minute. Therefore, we assumed a linear iodine uptake within the first 20 minutes for the time activity curve of the blood and the bi-exponential fits were performed from  $t=20$  min. The absorbed dose  $\bar{D}_{\text{bl}}(t)$  after 20 minutes was calculated as follows:

$$\bar{D}_{\text{bl}}(t) = A_0 \cdot \left( 108 \frac{\text{Gy} \cdot \text{ml}}{\text{GBq} \cdot \text{h}} \cdot \tau_{\text{ml of bl}}(t) + \frac{0.0188 \text{ Gy} \cdot \text{kg}^{\frac{2}{3}}}{wt^{\frac{2}{3}} \text{ GBq} \cdot \text{h}} \cdot \tau_{\text{tb}}(t) \right) \quad (1)$$

$A_0$  denotes the administered activity and  $wt$  represents the patient's weight in kg.

## 2.6 Statistical analysis

Data analysis and statistical evaluation was performed using Origin (OriginPro 2019, Origin Lab Corporation). To test whether data were distributed normally, the Shapiro-Wilk test was conducted. For comparing data sets the Wilcoxon signed-rank test was used for not normally distributed data and the paired sample t-test was used for normally distributed data. Results were considered as statistically significant for  $p < 0.05$ .

# 3. Results

## 3.1 Patients

For the ex-vivo study assessing the DNA damage induction and repair, 20 patients enrolled at UKW (IP1-IP18, WIP1 and WIP2) and 13 additional patients enrolled at UMR (MIP1-MIP13) for ablation treatment of differentiated thyroid cancer, who underwent their first radioiodine therapy according to the respective local standard of care, were included. The patients' pre-therapeutic blood samples, taken at UMR, were sent by courier immediately after withdrawal to UKW for further processing.

For the in-vivo study, 21 patients were enrolled at UKW, out of which 20 were eligible for the biodosimetry studies. For patient-related reasons, 2 patients (WIP1-WIP2) could not comply with the full biodosimetry protocol and were included only for the ex-vivo irradiation study. Therefore, 18 patients (IP1-IP18) participated in the full biodosimetry study (ex-vivo and in-vivo study). All patients were treated with  $^{131}\text{I}$ NaI according to the local standard of care. The mean activity administered to the 18 patients treated at UKW and enrolled in the full biodosimetry study was  $(3.6 \pm 0.1)$  GBq  $^{131}\text{I}$ NaI.

For easier handling of blood samples, the patient coding was adapted locally. Table 1 lists the respective internal and official MEDIRAD patient IDs and patient age and gender.

Table 1: Patient coding and demographic data.

Patient ID	Patient Age	In-Vivo Study	Patient Gender	
UKW internal	MEDIRAD			
IP1	UKW-001	44.7	Yes	female
IP2	UKW-002	65.3	Yes	female
IP3	UKW-003	24.9	Yes	female
IP4	UKW-004	28.6	Yes	female
IP5	UKW-005	55.2	Yes	female
IP6	UKW-006	21.0	Yes	female
IP7	UKW-007	54.7	Yes	female
IP8	UKW-010	48.8	Yes	female
IP9	UKW-011	45.1	Yes	female
IP10	UKW-012	44.6	Yes	female
IP11	UKW-013	59.9	Yes	male
IP12	UKW-014	26.2	Yes	female
IP13	UKW-015	36.3	Yes	male
IP14	UKW-016	38.9	Yes	female
IP15	UKW-017	54.8	Yes	male
IP16	UKW-018	63.8	Yes	female
IP17	UKW-020	19.8	Yes	male
IP18	UKW-021	59.2	Yes	female
WIP1	UKW-008	34.0	No	female
WIP2	UKW-009	61.0	No	female
MIP1	UMR-07	20.7	No	female
MIP2	UMR-06	25.9	No	male
MIP3	UMR-12	57.9	No	female
MIP4	UMR-13	36.6	No	male
MIP5	UMR-14	55.3	No	male
MIP6	UMR-15	67.0	No	male
MIP7	UMR-16	58.2	No	female
MIP8	UMR-17	33.6	No	female
MIP9	UMR-25	36.7	No	female
MIP10	UMR-26	37.1	No	female
MIP11	UMR-27	57.9	No	female
MIP12	UMR-29	31.1	No	female
MIP13	UMR-30	35.6	No	male

The mean age of the UKW patients participating in the biodosimetry study was ( $44 \pm 15$ ) years, for the UKM patients ( $43 \pm 15$ ) years. The age difference between the two groups was statistically not significant ( $p < 0.05$ ). 9 male patients and 24 female patients were included in the study (see table 1). A retrospective analysis of the patient data revealed that, due to technical difficulties with blood preparation and foci counting, patient MIP3 had to be excluded from further analysis.

### 3.2 Ex-vivo data on DNA damage induction and repair

The median of the number of foci per cell at  $t = 0$  h (repair time  $0$  h = d) was 0.38 (min: 0.20, max: 0.86) and the mean number of foci per cell were  $0.46 \pm 0.17$  after 4 h repair time, and  $0.44 \pm 0.16$  after 24 h for the baseline values. After irradiation, the mean values were ( $1.13 \pm 0.22$ ) (d), ( $0.72 \pm 0.16$ ) (repair time 4 h), and ( $0.48 \pm 0.16$ ) (repair time 24 h) foci per cell [7]. The mean absorbed dose in all samples internally irradiated ex vivo was ( $50.1 \pm 2.3$ ) mGy.

All foci values (baseline and irradiated) were normally distributed except the baseline value after direct fixation ( $0$  h = d). The baseline values (d vs. 24 h and 4 h vs. 24 h) were statistically not different,



whereas the d vs. 4 h comparison revealed a significant difference. This variability for the baseline samples can be explained by the influence of counting statistics.

The average number of foci per cell of the irradiated samples was significantly higher than the baseline values at all time points when compared to baseline. This was the case even for  $t = 24$  h ( $p < 0.0059$ ). For all irradiated samples (d, 4 h, 24 h post irradiation) there was a significant difference of the average numbers of foci per cell [7].

Figure 1 shows the average number of RIF per cell at the nominal time points (d, 4 h, and 24 h) for patients IP1-IP18, WIP1, WIP2, MIP1, MIP2, and MIP4-MIP13. The average RIF per cell after internal ex vivo irradiation with a nominal absorbed dose of 50 mGy is  $(0.72 \pm 0.16)$  RIF per cell. This value is, within the respective uncertainties, in good agreement with the expected value of  $(0.77 \pm 0.03)$  RIF per cell calculated with the calibration curve provided by Eberlein et al [8]. At  $t = 4$  h, the mean value of the average number of RIF per cell was  $(0.26 \pm 0.09)$  RIF per cell, and at  $t = 24$  h  $(0.04 \pm 0.09)$  RIF per cell.

A monoexponential fit, comprising the three mean values of the average RIF per cell for each time point, results in a decay rate of  $(0.25 \pm 0.05) \text{ h}^{-1}$ . For deriving the fraction for unrepaired foci, a combined fit of a monoexponential function combined with an offset describing the unrepaired fraction of foci through all data points (including all individual RIF values of all patients) was performed. The resulting repair rate was  $(0.28 \pm 0.03) \text{ h}^{-1}$ , and the value for the offset was  $(0.06 \pm 0.02)$  RIF per cell. This observation of an offset larger than 0 is in agreement with our finding of a statistically significant elevated average number of foci per cell of the irradiated samples at  $t = 24$  h. This value corresponds to about 6 % unrepaired RIF per cell 24 h after irradiation.

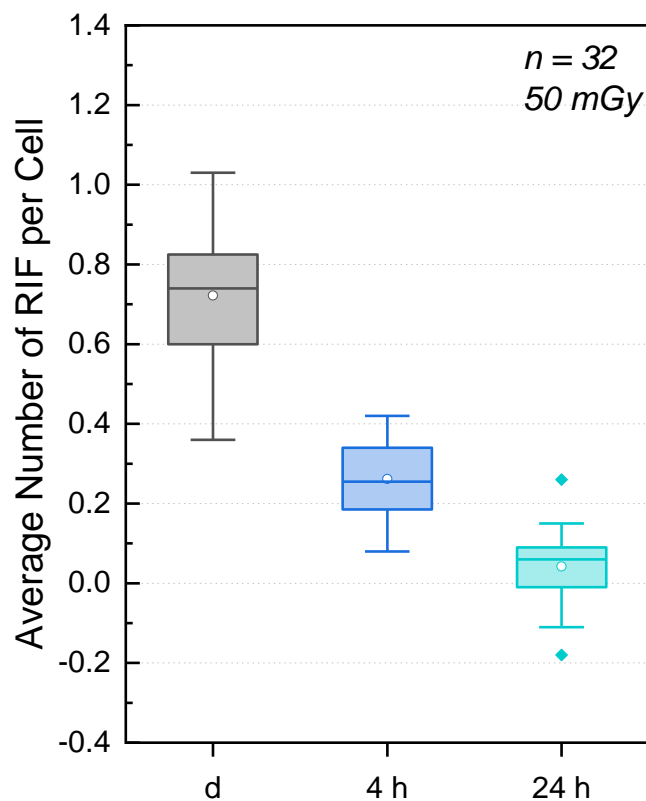


Figure 1: Box plot of the average number of RIF per cell immediately after, 4 h and 24 h after ex-vivo irradiation with 50 mGy. The boxes comprise the 2<sup>nd</sup> and 3<sup>rd</sup> quartile of the data, the horizontal line defines the median and the circle the mean. Outliers ( $> 1.5 \times \text{IQR}$  (interquartile range)) are marked by filled diamonds.

The mean value of the individual fits for the RIF decay rate  $R$  of  $(0.25 \pm 0.10) \text{ h}^{-1}$  obtained by this study is slightly lower than the values of  $0.29 \text{ h}^{-1}$  and  $0.35 \text{ h}^{-1}$  for lymphocytes, that were irradiated externally with X-rays with absorbed doses of 20 mGy and 100 mGy, respectively (calculated from the data of 23 patients taken from Fig 5. of Löbrich et al. [9]), and the value of  $0.35 \text{ h}^{-1}$  determined by Horn et al. for absorbed doses  $\geq 0.5 \text{ Gy}$  [10] (data of 21 healthy donors). Beels et al. [11] reported, for three volunteers whose samples were irradiated with 0.2 Gy X-rays and  $\gamma$ -rays, a value for the decay rate of  $0.25\text{-}0.29 \text{ h}^{-1}$ . This value is in the same range as the results provided in this study. Our results are also in agreement with the cell culture data on fibroblasts by Mariotti et al. [12] at higher absorbed doses (1-2 Gy) of  $0.23 \text{ h}^{-1}$ . Yin et al. observed, after irradiating blood samples of 11 patients with absorbed doses of 0.5 Gy and more, a repair rate of  $(0.277 \pm 0.014) \text{ h}^{-1}$  before radiotherapy and  $(0.293 \pm 0.011) \text{ h}^{-1}$  for blood samples taken 1 hour after irradiation, a value that is also in close agreement with our findings [7].

### 3.3 In-vivo data on DNA damage induction and repair in patients

#### 3.3.1 Blood-based dosimetry

For all of the 18 UKW patients included in the full in vivo biodosimetry study (IP1-IP18), dosimetry data according to the methodology described by the EANM SOP [4] were generated. The mean activity administered to the patients was  $(3.6 \pm 0.1) \text{ GBq}$ . The mean total absorbed dose to the blood of these patients was  $(316 \pm 86) \text{ mGy}$ . If patient IP15 with an unusual temporal pattern of the time-activity curve 48 h after administration of the activity and a high total absorbed dose to the blood of 605 mGy is excluded, the mean total absorbed dose to the blood was reduced to  $(299 \pm 49) \text{ mGy}$ . The absorbed doses to the blood determined in this study are in good agreement to those obtained in previous studies (see e.g. [5, 13-15]). Table 2 displays the mean absorbed doses to the blood at the nominal time points of blood sampling.

Table 2: Mean values of absorbed doses and dose rates to the blood at the nominal time points of blood sampling.

Nominal Time after administration (h)	Mean Absorbed Dose to the Blood (mGy)	Mean Absorbed Dose Rate to the Blood (mGy/h)
1	$14 \pm 3$	$15.7 \pm 2.9$
2	$30 \pm 4$	$14.8 \pm 1.8$
3	$44 \pm 6$	$13.8 \pm 1.8$
4	$57 \pm 7$	$12.7 \pm 1.8$
24	$197 \pm 27$	$3.6 \pm 0.8$
48	$247 \pm 37$	$1.1 \pm 0.4$
96	$279 \pm 43$	$0.3 \pm 0.2$
168	$297 \pm 55$	$0.1 \pm 0.1$ (without IP 15)
<b>Total</b>	$299 \pm 49$ (without IP15)	-

### 3.3.2 DNA damage induction and repair

The average number of RIF per cell after administration of  $^{131}\text{I}$  in 18 UKW patients (IP1-IP18) is shown in Figure 2 as a box plot, including the data points and the corresponding fit of a normal distribution (black dotted line) for each nominal time point. The average number of RIF per cell increased in the first hours after therapy, declining at later time points. The actual time points differed slightly because of variations in the individual patient management. The mean number of RIF per cell varied between  $(0.63 \pm 0.18, n=18)$  at 4 h,  $(0.43 \pm 0.20, n=18)$  at 24 h,  $(0.28 \pm 0.17, n=18)$  at 48 h,  $(0.14 \pm 0.14, n = 12)$  at 96 h, and  $(0.06 \pm 0.18, n = 17)$  at 168 h after administration of  $^{131}\text{I}$ .

At all nominal time points (except for  $t = 3$  h), the data follow a normal distribution. The variability of the RIF at the different time points can be explained by the individual biokinetics of radioiodine in patients after administration, thus leading to individual differences in focus induction, and by slight time differences between the actual and the nominal time points of the blood withdrawal. The mean values of all data sets for the time points 4 h after administration or later with 17 or more data points (except  $t = 96$  h, for which only 12 valid data points were available) decreased significantly. After 168 h the repair was complete in almost all patients. The time course is similar to those that we observed in previous studies in patients either after therapy with  $^{131}\text{I}$  [5] or  $^{177}\text{Lu}$  [2, 16].

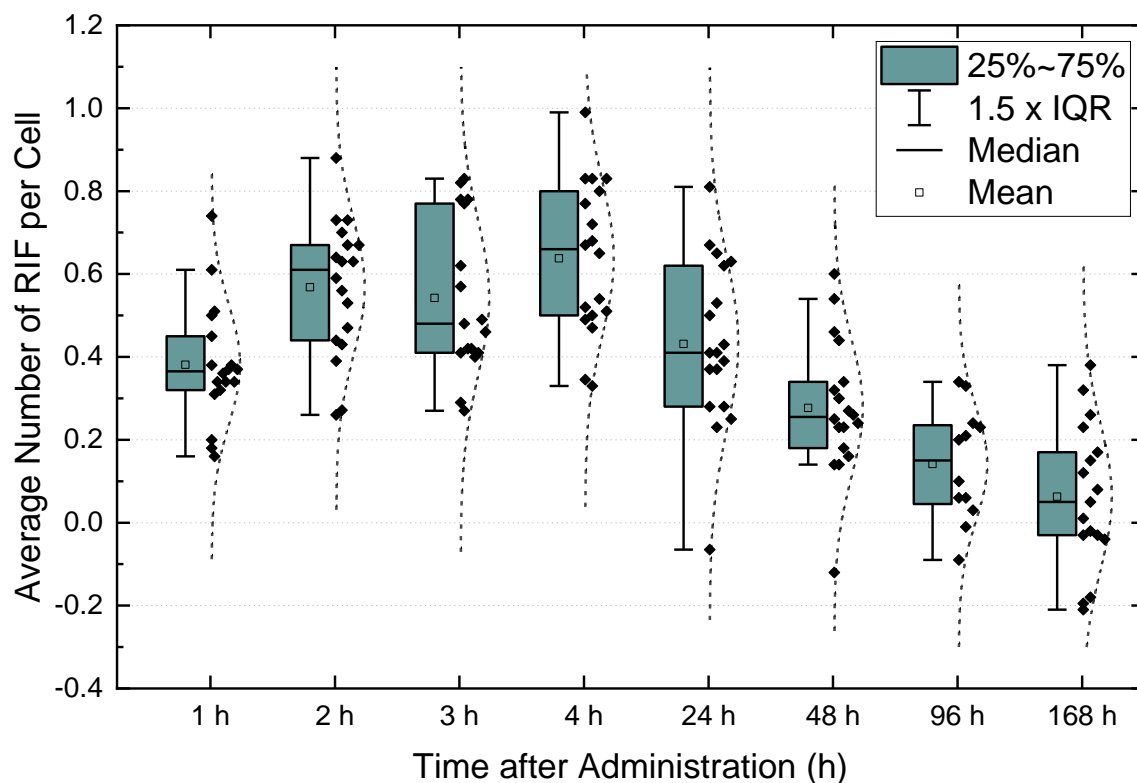


Figure 2: Time course of the average number of RIF per cell after administration of  $^{131}\text{I}$  in 18 patients IP1-IP18 shown as a box plot including the data points and the corresponding fit of a normal distribution as a black dotted line.

Figure 3 shows the average number of RIF per cell as a function of the absorbed dose to the blood after radioiodine administration. In order to model the induction of foci in the first four hours after administration, the data were approximated by a linear fit. The resulting slope was  $(0.0101 \pm 0.008) \text{ mGy}^{-1}$  with an intercept of  $(0.1002 \pm 0.0273)$  ( $R^2 = 0.64$ ). The shaded area in figure 3 represents the 95% confidence band. These values are in good agreement with those of our previous publication for patients after radioiodine therapy with a slope of  $(0.0117 \pm 0.0006) \text{ mGy}^{-1}$  and an intercept of  $(0.0064 \pm 0.0089)$  [5].

At later time points ( $\geq 24 \text{ h}$ ), the dependency of the average number of foci per cell on the absorbed dose is characterized by the on-going repair competing with the induction of new foci by the still increasing absorbed doses with diminishing absorbed dose rates, which are different for each patient. This is the reason why the number of RIF decrease, although the absorbed dose to the blood increases. Patients with high absorbed doses (e.g. IP3 or IP15) still show a higher number of RIF as compared to the other patients. To illustrate the dependency on the absorbed dose rate at these later time points, figure 4 shows a linear fit of the RIF as a function of the absorbed dose rate for the nominal time points 24 h or later. The slope of the fit is  $(0.097 \pm 0.012) \text{ h mGy}^{-1}$  and the y-axis intercept is  $(0.085 \pm 0.024)$  ( $R^2 = 0.49$ ). A similar observation was made in our earlier study with  $^{177}\text{Lu}$ -PSMA-treated patients [16]. A potential conclusion could be that even at low dose rates new foci are induced and, therefore, the reduction pattern of RIF at later time points is altered and, therefore, does not reflect solely the repair.

In general, some variability could be observed between individual patients. However, as the the distribution of the patient data (absorbed doses and average number of RIF) mostly followed a normal distribution, no patients could be identified showing any striking deviation in foci induction and repair.

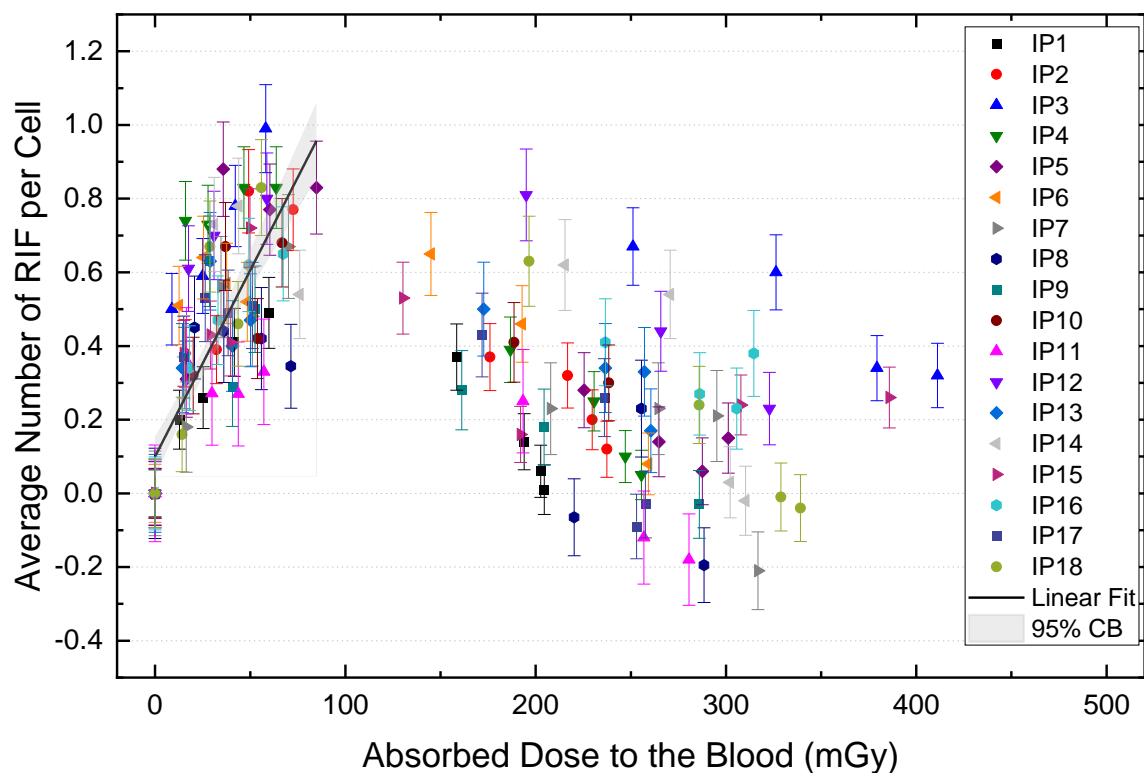


Figure 3: Average number of RIF/cell as a function of the absorbed dose to the blood. For the time points up to 5 h after administration a linear fit is denoted by a straight line (grey area: 95 % confidence band (CB)).

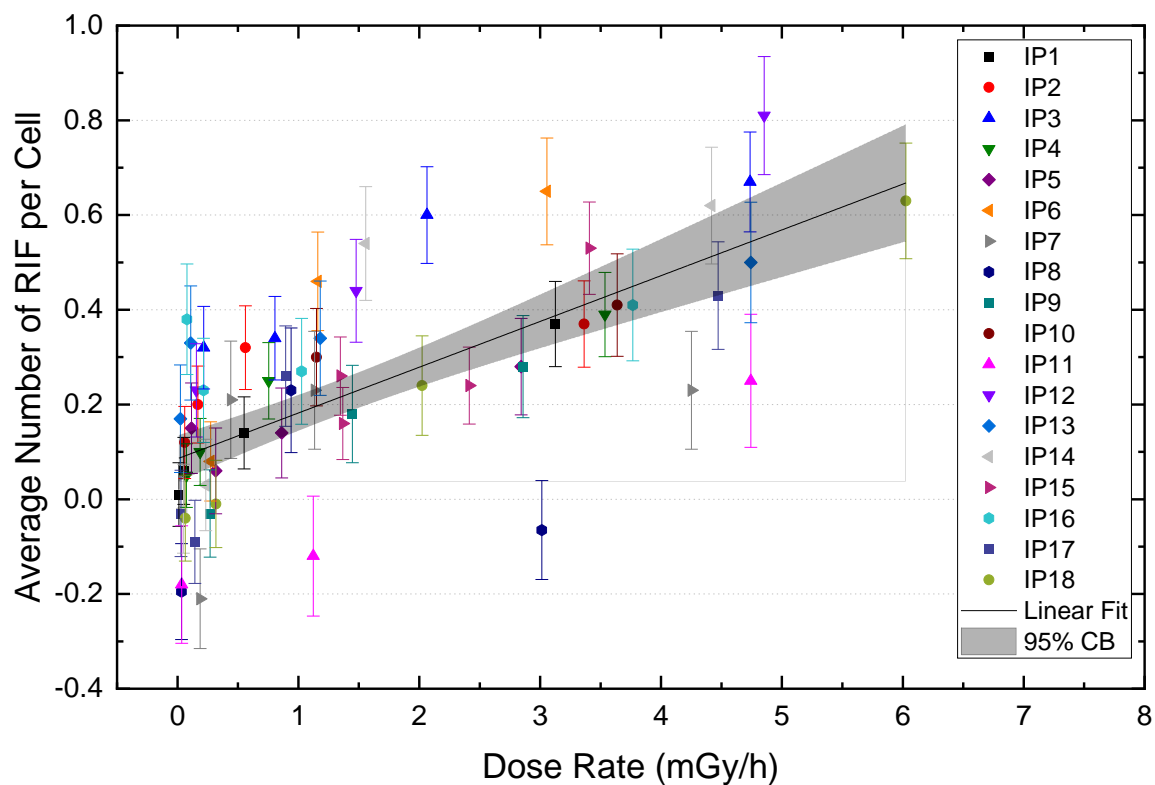


Figure 4: Average number of RIF per cell at time points  $\geq 24$  h as a function of the absorbed dose rate to the blood. A linear fit is denoted by a straight line (grey area: 95 % confidence band (CB)).

### 3.3.3 Comparison of ex-vivo and in-vivo repair

For directly comparing the temporal pattern of DNA damage repair between the ex-vivo study and the in-vivo study, the corresponding results of the 18 UKW patients were compared (IP1-IP18). The mean absorbed dose of the respective 18 ex-vivo irradiated samples was  $(49.7 \pm 2.4)$  mGy.

Figure 5 shows a comparison of the ex-vivo (panel A) and in-vivo (panel B) repair dynamics as a function of time after irradiation (ex vivo) or radioiodine administration (in vivo) for the 18 UKW patients. For all time points of the ex-vivo study (0 h (d), 4 h, 24 h), the mean average number of RIF per cell after irradiation was  $0.65 \pm 0.18$  at  $t = 0$  h (d),  $0.25 \pm 0.09$  at  $t = 4$  h, and  $0.06 \pm 0.09$  at  $t = 24$  h. For the nominal time points of the in-vivo study (1 h, 4 h, 24 h after radioiodine administration), the mean average number of RIF per cell was  $0.38 \pm 0.14$  at  $t = 1$  h,  $0.64 \pm 0.18$  at  $t = 4$  h, and  $0.43 \pm 0.20$  at  $t = 24$  h.

The mean absorbed dose of the patients included in the study at the actual time of measurements was  $(16 \pm 3)$  mGy at  $t = 1$  h,  $(62 \pm 10)$  mGy at  $t = 4$  h, and  $(191 \pm 32)$  mGy at  $t = 24$  h. Comparing the ex-vivo average number of RIF per cell for similar absorbed doses observed in vivo (ex vivo: 50 mGy, in vivo: 62 mGy) provides comparable mean values of the average numbers of RIF per cell which are statistically not different ( $p=0.78$ ). This comparison shows that the induction of RIF is similar for the ex-vivo and the in-vivo study. The main difference in the repair kinetics can be attributed to the non-negligible dose rate at late time points observed in patients which is also illustrated by figure 4.

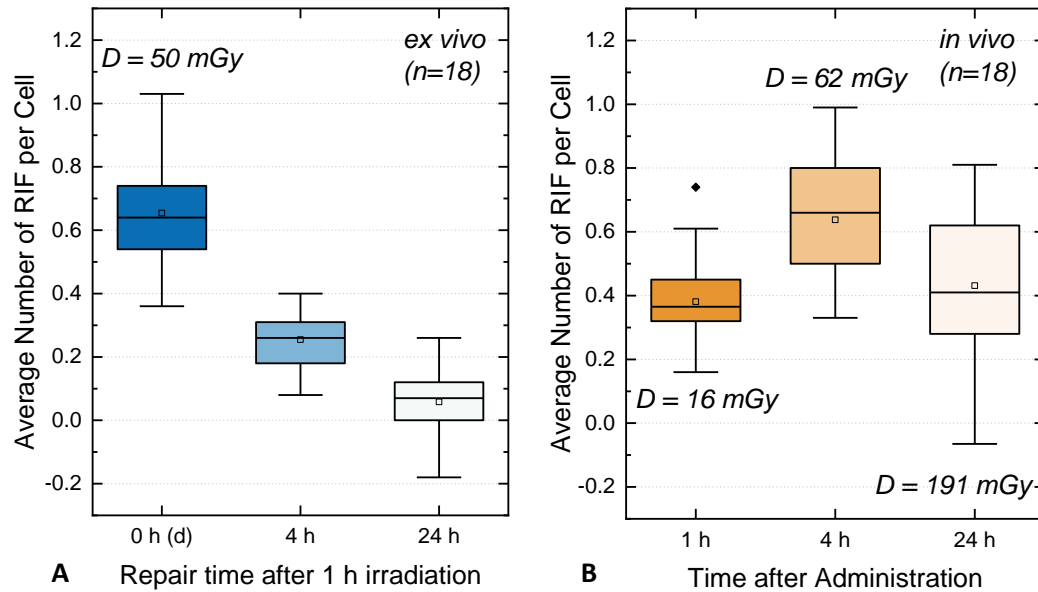


Figure 5: Comparison of the ex vivo (left panel A) and in vivo (right panel B) repair dynamics as a function of time after irradiation (ex vivo) or radioiodine administration (in vivo). In addition, panel B shows the mean absorbed doses to the blood at the nominal time points. The boxes comprise the 2<sup>nd</sup> and 3<sup>rd</sup> quartile of the data, the horizontal line defines the median and the circle the mean. Outliers (> 1.5 x IQR) are marked by filled diamonds.

## 4. Conclusion

Our data show that the ex vivo DNA damage repair of PBMCs in 32 patients - quantified by the DNA damage assay - after an internal irradiation of blood with low dose rates follows similar patterns noted after external irradiation with comparable or higher dose rates. DNA damage is efficiently repaired, with a repair rate comparable to that of external irradiation with  $\gamma$ - or X-rays. About 6 % of the initial average RIF per cell remain unrepaired 24h after ex vivo internal irradiation.

In vivo, the pattern of DNA damage induction and repair observed in 18 patients after radioiodine therapy is different due to the slow increase of the absorbed doses over time (about 2/3 of the total absorbed dose to the blood are imparted in the first 24 h after administration of the radiopharmaceutical), and the variable and decreasing dose rates. As shown in previous studies, we observe a linear increase of the average number of RIF per cell up to 4 h after radioiodine administration with a slope that is comparable to that of the ex-vivo irradiation, and, in contrast to the ex-vivo study, incomplete repair after 24 h, highlighting different conditions in the cell culture and in patients. In vivo, there was continuous irradiation of blood following the administration of  $^{131}\text{I}$  for the treatment of thyroid cancer with decreasing, however, still relevant absorbed dose rates in patients  $\geq 24$  h after administration. This leads to altered DNA damage repair kinetics in vivo, most likely due to dwindling DSB induction competing with DSB repair. At these late time points, the DNA damage repair still competes with the induction of DSBs and thus foci, which is illustrated by the linear dependency of the average number of RIF per cell as a function of the absorbed dose rate. In most patients, 168 h after administration of radioiodine, the DNA damage is no longer detectable, indicating effective DSB repair in the PBMCs.

## 5. References

1. TNM Classification of Malignant Tumours, 8th Edition: Wiley-Blackwell; 2016.
2. Eberlein U, Nowak C, Bluemel C, Buck AK, Werner RA, Scherthan H, et al. DNA damage in blood lymphocytes in patients after  $^{177}\text{Lu}$  peptide receptor radionuclide therapy. *Eur J Nucl Med Mol Imaging*. 2015;42:1739-49. doi:10.1007/s00259-015-3083-9.
3. Lamkowski A, Forcheron F, Agay D, Ahmed EA, Drouet M, Meineke V, et al. DNA damage focus analysis in blood samples of minipigs reveals acute partial body irradiation. *PLoS One*. 2014;9:e87458. doi:10.1371/journal.pone.0087458.
4. Lassmann M, Hänscheid H, Chiesa C, Hindorf C, Flux G, Luster M. EANM Dosimetry Committee series on standard operational procedures for pre-therapeutic dosimetry I: blood and bone marrow dosimetry in differentiated thyroid cancer therapy. *Eur J Nucl Med Mol Imaging*. 2008;35:1405-12. doi:10.1007/s00259-008-0761-x.
5. Eberlein U, Scherthan H, Bluemel C, Peper M, Lapa C, Buck AK, et al. DNA Damage in Peripheral Blood Lymphocytes of Thyroid Cancer Patients After Radioiodine Therapy. *J Nucl Med*. 2016;57:173-9. doi:10.2967/jnumed.115.164814.
6. Leggett RW. A physiological systems model for iodine for use in radiation protection. *Radiat Res*. 2010;174:496-516. doi:10.1667/RR2243.1.
7. Schumann S, Scherthan H, Pfestroff K, Schoof S, Pfestroff A, Hartrampf P, et al. DNA damage and repair in peripheral blood mononuclear cells after internal ex vivo irradiation of patient blood with  $^{131}\text{I}$  Eur J Nucl Med Mol Imaging. 2021;under revision.
8. Eberlein U, Peper M, Fernandez M, Lassmann M, Scherthan H. Calibration of the gamma-H2AX DNA double strand break focus assay for internal radiation exposure of blood lymphocytes. *PLoS One*. 2015;10:e0123174. doi:10.1371/journal.pone.0123174.
9. Löbrich M, Rief N, Kuhne M, Heckmann M, Fleckenstein J, Rube C, et al. In vivo formation and repair of DNA double-strand breaks after computed tomography examinations. *Proc Natl Acad Sci U S A*. 2005;102:8984-9.
10. Horn S, Barnard S, Rothkamm K. Gamma-H2AX-based dose estimation for whole and partial body radiation exposure. *PLoS One*. 2011;6:e25113. doi:10.1371/journal.pone.0025113.
11. Beels L, Werbrouck J, Thierens H. Dose response and repair kinetics of gamma-H2AX foci induced by in vitro irradiation of whole blood and T-lymphocytes with X- and gamma-radiation. *Int J Radiat Biol*. 2010;86:760-8. doi:10.3109/09553002.2010.484479.
12. Mariotti LG, Pirovano G, Savage KI, Ghita M, Ottolenghi A, Prise KM, et al. Use of the gamma-H2AX assay to investigate DNA repair dynamics following multiple radiation exposures. *PLoS One*. 2013;8:e79541. doi:10.1371/journal.pone.0079541.
13. Hänscheid H, Lassmann M, Luster M, Thomas SR, Pacini F, Ceccarelli C, et al. Iodine biokinetics and dosimetry in radioiodine therapy of thyroid cancer: procedures and results of a prospective international controlled study of ablation after rhTSH or hormone withdrawal. *J Nucl Med*. 2006;47:648-54.
14. Lassmann M, Hänscheid H, Gassen D, Biko J, Meineke V, Reiners C, et al. In vivo formation of gamma-H2AX and 53BP1 DNA repair foci in blood cells after radioiodine therapy of differentiated thyroid cancer. *J Nucl Med*. 2010;51:1318-25. doi:10.2967/jnumed.109.071357.
15. Verburg FA, Lassmann M, Mader U, Luster M, Reiners C, Hänscheid H. The absorbed dose to the blood is a better predictor of ablation success than the administered  $^{131}\text{I}$  activity in thyroid cancer patients. *Eur J Nucl Med Mol Imaging*. 2011;38:673-80. doi:10.1007/s00259-010-1689-5.
16. Schumann S, Scherthan H, Lapa C, Serfling S, Muhtadi R, Lassmann M, et al. DNA damage in blood leucocytes of prostate cancer patients during therapy with  $^{177}\text{Lu}$ -PSMA. *Eur J Nucl Med Mol Imaging*. 2019;46:1723-32. doi:10.1007/s00259-019-04317-4.